Metric-space analysis of systems immersed in a magnetic field

P. M. Sharp[*] and I. D'Amico[†]

Department of Physics and York Centre for Quantum Technologies, University of York, York YO10 5DD, United Kingdom
(Received 25 April 2015; published 18 September 2015)

Understanding the behavior of quantum systems subject to magnetic fields is of fundamental importance and underpins quantum technologies. However, modeling these systems is a complex task, because of many-body interactions and because many-body approaches such as density-functional theory get complicated by the presence of a vector potential into the system Hamiltonian. We use the metric-space approach to quantum mechanics to study the effects of varying the magnetic vector potential on quantum systems. The application of this technique to model systems in the ground state provides insight into the fundamental mapping at the core of current density-functional theory, which relates the many-body wave function, particle density, and paramagnetic current density. We show that the role of the paramagnetic current density in this relationship becomes crucial when considering states with different magnetic quantum numbers m. Additionally, varying the magnetic field uncovers a richer complexity for the "band structure" present in ground-state metric spaces, as compared to previous studies varying scalar potentials. The robust nature of the metric-space approach is strengthened by demonstrating the gauge invariance of the related metric for the paramagnetic current density. We go beyond ground-state properties and apply this approach to excited states. The results suggest that, under specific conditions, a universal behavior may exist for the relationships between the physical quantities defining the system.

I. INTRODUCTION

Systems immersed in magnetic fields are a fundamental research topic, as is the case, for example, for atoms immersed in strong fields [1,2], and are also an integral part of emerging quantum technologies, such as quantum computation, which utilize quantum systems controlled or otherwise affected by magnetic fields. For example, the inhomogeneous magnetic field generated by the nuclei's spins decreases quantum coherence of electron-spin qubits in III–V quantum dots [3], while full polarization of the spin bath through an applied magnetic field suppresses electron-spin decoherence in nitrogen-vacancy centers and nitrogen impurities in diamond [4]. Understanding systems immersed in a magnetic field at a quantum level is therefore of both fundamental and technological importance.

However, the presence of a magnetic field introduces additional complexity to the system's Hamiltonian. In fact, as opposed to a confining potential, which is defined by a scalar potential $V(\mathbf{r})$, the magnetic field is defined by $\mathbf{B}(\mathbf{r}) = \nabla \times \mathbf{A}(\mathbf{r})$, where $\mathbf{A}(\mathbf{r})$ is a *vector* potential. To account for its presence, density-functional theory (DFT) must be extended to current-density-functional theory (CDFT). In this paper we will use the metric-space approach to quantum mechanics [5–8] to study the effect on quantum systems of changing the vector potential and we will carefully consider the implications of the results for CDFT. This is particularly relevant as there are still open questions with respect to the fundamentals of this theory (see, for example, Refs. [9–13]).

The metric-space approach involves the derivation of "natural" metrics from conservation laws to assign a distance between two physically relevant functions [8]. In recent work these metrics were applied to the basic variables of both standard DFT [5–7,14] and CDFT [8]. In Refs. [5,8] it was demonstrated that the core theorems of DFT and CDFT, respectively, indeed represent mappings between metric spaces: This helps understanding the power of the metric-space approach and why its use has already allowed for the discovery of additional properties of these core theorems. The results in Ref. [8], pertaining to systems with fixed magnetic fields, considered only the effects of varying the scalar potential; in this paper we demonstrate how the metric-space approach to quantum mechanics can be applied to analyze systems while varying the vector potential and hence the magnetic field.

A significant issue for any theory involving magnetic fields is gauge transformations of the scalar and vector potentials. The magnetic field, along with all physical observables, is gauge invariant. Hence, in order to properly describe the distances between physical quantities, the metrics we derive must be robust against gauge transformations. However, quantities such as the wave function and the paramagnetic current density are gauge variant and changes in the vector potential can result in gauge transformations for these quantities. Thus, here we will extend the metric-space approach to ensure that the metrics associated with these quantities are gauge invariant.

We will provide further insight into the fundamental mappings between key physical quantities at the core of CDFT by studying the ground state of model systems as the vector potential is varied. In particular we will examine how the "band structure" introduced into ground-state metric spaces by the presence of a magnetic field [8] responds to changes in the field. To complement this picture, we will apply the metric-space approach to quantum mechanics to explore the properties of excited states. Results will also help with validating the conclusions from the ground-state analysis.

The rest of this paper is organized as follows. In Sec. II we briefly review how functions obeying integral conservation laws can be cast as metric spaces and the application of this approach to the wave function, particle density, and paramagnetic current density. Section III demonstrates how

---

[*]pms510@york.ac.uk
[†]irene.damico@york.ac.uk

the gauge properties of the paramagnetic current density are accounted for when forming the related metric space in order to ensure that the metric is gauge invariant. In Sec. IV we examine how the "band structure" present in metric spaces for ground states is affected by variations in the magnetic field and the relevance of this for CDFT. Section V goes beyond ground states. In Sec. VI we present a summary and our conclusions. We use atomic units $\hbar = e = m_e = 1/4\pi\epsilon_0 = 1$ throughout this paper.

II. METRIC SPACES FOR PHYSICAL FUNCTIONS

In Ref. [8] a general procedure for deriving metric spaces from conservation laws was presented. For completeness in this section we briefly review this procedure and the properties of these metric spaces.

A metric space (X,D) consists of a nonempty set of points X and a metric $D : X \times X \to \mathbb{R}$, which assigns a distance between any two elements of X. For all $a,b,c \in X$ the metric must satisfy the following axioms [15,16]:

$$D(a,b) \geqslant 0, \quad D(a,b) = 0 \Leftrightarrow a = b, \quad (1)$$

$$D(a,b) = D(b,a), \quad (2)$$

$$D(a,b) \leqslant D(a,c) + D(c,b). \quad (3)$$

These axioms are known as positivity, symmetry, and the triangle inequality, respectively.

Consider now a conservation law of the form

$$\int |f(\mathbf{x})|^p d\mathbf{x} = c, \quad (4)$$

with c a finite positive constant and $\mathbf{x} = (x_1, \ldots, x_N)$ including any spatial or spin coordinate in any dimensionality. Then for each p such that $1 \leqslant p < \infty$, the entire set of functions that satisfies Eq. (4) forms an L^p vector space. Then the corresponding metric

$$D_f(f_1,f_2) = \left[\int |f_1(\mathbf{x}) - f_2(\mathbf{x})|^p d\mathbf{x} \right]^{1/p} \quad (5)$$

also applies to the *restricted* set of *physical* functions obeying the conservation law (4) [8]. As c spans the set of its physically allowed values $\{c_i\}$, the metric (5) imposes on its metric space an "onion-shell" geometry that consists of a series of concentric spheres with radii $c_i^{1/p}$, as sketched in Fig. 1.

We note that the procedure developed in Ref. [8] can be extended to conservation laws of the form

$$\sum_{i=1}^{n} |f_i|^p = c, \quad (6)$$

as the l^p vector spaces for sums are directly analogous to the L^p spaces for integrals [16]. In this case the induced metric will be

$$D_f(f_1,f_2) = \left[\sum_{i=1}^{n} |f_{1_i} - f_{2_i}|^p \right]^{1/p}. \quad (7)$$

Thus, we have a general procedure to construct a metric for any conservation law that is, or can be cast, in the form of
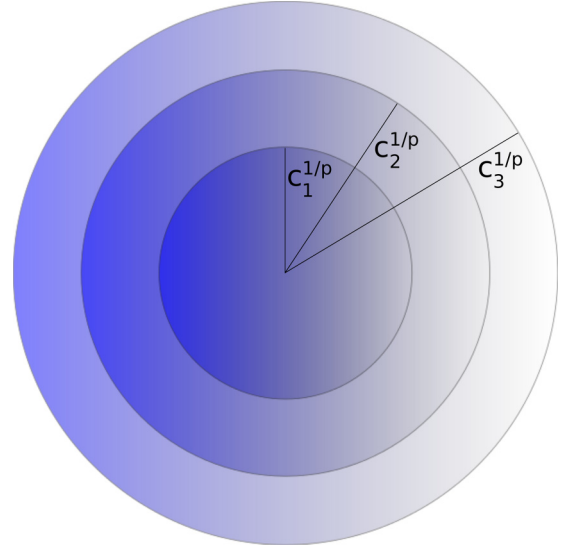

FIG. 1. (Color online) Sketch of the structure of the "onion-shell" geometry, consisting of a series of concentric spheres. The first three spheres are shown, with radii $c_i^{1/p}$, $i = 1,2,3$.

Eq. (4) or (6). We can therefore state that such conservation laws induce metrics on the set of related physical functions. As they descend directly from conservation laws, these "natural" metrics are nontrivial and contain the relevant physics.

Following this procedure the metrics

$$D_\psi(\psi_1,\psi_2) = \left[\int \left(|\psi_1|^2 + |\psi_2|^2 \right) d\mathbf{r}_1 \cdots d\mathbf{r}_N \right.$$
$$\left. - 2 \left| \int \psi_1^* \psi_2 d\mathbf{r}_1 \cdots d\mathbf{r}_N \right| \right]^{1/2}, \quad (8)$$

$$D_\rho(\rho_1,\rho_2) = \int |\rho_1(\mathbf{r}) - \rho_2(\mathbf{r})| d\mathbf{r}, \quad (9)$$

$$D_{\mathbf{j}_{p_\perp}}(\mathbf{j}_{p_1},\mathbf{j}_{p_2}) = \int \left| \left\{ \mathbf{r} \times [\mathbf{j}_{p_1}(\mathbf{r}) - \mathbf{j}_{p_2}(\mathbf{r})] \right\}_z \right| d\mathbf{r} \quad (10)$$

for wave functions ψ [5], particle densities ρ [5], and paramagnetic current densities $\mathbf{j}_p = (j_{p_x}, j_{p_y}, j_{p_z})$ [8] have been introduced. These metrics follow from, respectively, the conservation of wave-function norm, of particle number, and of the z component of the angular momentum; the latter can be expressed as Eq. (4), when using the relation [8]

$$\int [\mathbf{r} \times \mathbf{j}_p(\mathbf{r})]_z d\mathbf{r} = \langle \psi | \hat{L}_z | \psi \rangle = m. \quad (11)$$

For paramagnetic current densities, Eq. (11) directly imposes an equivalence relation on the set of all paramagnetic current densities because $[\mathbf{r} \times \mathbf{j}_p(\mathbf{r})]_z$ is independent of j_{p_z}. As a result, $D_{\mathbf{j}_{p_\perp}}$ is a metric defined on a set of equivalence classes of paramagnetic current densities, with the classes characterized by paramagnetic current densities with the same transverse component $\mathbf{j}_{p_\perp} = (j_{p_x}, j_{p_y})$.

The radii of the concentric spheres in the "onion-shell" geometry of the aforementioned metric spaces are $\sqrt{N}$ for

the wave-function metric space,[1] N for the particle density metric space, and $|m|$ for the paramagnetic current density metric space [5,8]. When considering individual spheres, the diameter of the sphere imposes an upper bound on the value of the distance.

III. GAUGE INVARIANCE OF METRICS

When dealing with electromagnetic fields, it is important to consider the choice of gauge. The scalar and vector potentials in the Hamiltonian are not unique, as a change of gauge transforms the potentials according to

$$V'(\mathbf{r}) = V(\mathbf{r}) + c', \quad \mathbf{A}'(\mathbf{r}) = \mathbf{A}(\mathbf{r}) - \nabla\chi, \quad (12)$$

where c' is a constant and $\chi(\mathbf{r})$ is a scalar field [17]. These transformations preserve the electromagnetic fields and all physical observables.

With regard to the quantities we consider in this paper, the particle density is gauge invariant, but the wave function and paramagnetic current density are not. After a change of gauge, the wave function undergoes a unitary transformation, which is given by [18]

$$\psi'(\mathbf{r}) = e^{[i\chi(\mathbf{r})]}\psi(\mathbf{r}). \quad (13)$$

The paramagnetic current density transforms according to [17]

$$\mathbf{j}'_p(\mathbf{r}) = \mathbf{j}_p(\mathbf{r}) + \rho(\mathbf{r})\nabla\chi. \quad (14)$$

Thus, when considering changes in the vector potential, we must be aware of the effect of gauge transformations on the physical quantities we are considering. Our metrics are constructed to provide nontrivial information that is physically relevant; they are based in fact on conservation laws. It is paramount then that they are also gauge invariant. The issue of ensuring that the wave-function metric is gauge invariant has been discussed in Ref. [5]; we provide a formal review of the approach in Appendix A. In this paper we wish to discuss gauge invariance with respect to the paramagnetic current density metric.

Gauge invariance for the paramagnetic current density metric

To consider the gauge properties of $D_{\mathbf{j}_{p\perp}}(\mathbf{j}_{p_1},\mathbf{j}_{p_2})$, first of all we require that $\mathbf{j}_{p_1}(\mathbf{r})$ and $\mathbf{j}_{p_2}(\mathbf{r})$ are within the same gauge. Then, applying the gauge transformation (14), we obtain

$$D_{\mathbf{j}_{p\perp}}(\mathbf{j}'_{p_1},\mathbf{j}'_{p_2}) = \int \left|\left\{\mathbf{r} \times \left[\mathbf{j}'_{p_1}(\mathbf{r}) - \mathbf{j}'_{p_2}(\mathbf{r})\right]\right\}_z\right| d\mathbf{r},$$

$$= \int \left|\left(\mathbf{r} \times \left\{\mathbf{j}_{p_1}(\mathbf{r}) - \mathbf{j}_{p_2}(\mathbf{r})\right.\right.\right.$$
$$\left.\left.\left. + [\rho_1(\mathbf{r}) - \rho_2(\mathbf{r})]\nabla\chi\right\}\right)_z\right| d\mathbf{r}. \quad (15)$$

Equation (15) states that, in general, the paramagnetic current density distance defined by Eq. (10) is modified by a gauge transformation. This seems to contradict the fact that we base our metrics on conservation laws, which must be gauge invariant. In order to reconcile this apparent contradiction let

---

[1]We follow the same convention as Ref. [5], where wave functions are normalized to the particle number N.

us explore more closely which quantities are gauge variant and which are the ones that must be conserved.

With reference to Eq. (11), the measurable physical quantity that must be conserved by gauge transformations is m, which, in the gauge chosen, corresponds to the component $\hat{L}_z$ of the angular momentum. However, it is crucial to note that $\hat{L}_z$ is not (nor need be) gauge invariant.

In fact, the operator $\hat{L}_z$ is defined as

$$\hat{L}_z = \sum_{i=1}^{N} [\mathbf{r}_i \times \hat{\mathbf{p}}_i]_z, \quad (16)$$

where $\hat{\mathbf{p}}$ is the canonical linear momentum $\hat{\mathbf{p}} = -i\nabla$. Although $\mathbf{r}$ is gauge invariant, $\hat{\mathbf{p}}$ is gauge variant and therefore so is $\hat{L}_z$. In the following we wish to extend Eq. (10) so that the metric associated with the conservation of m is indeed gauge invariant.

We consider a system for which there exists at least one gauge such that $[\hat{L}_z, \hat{H}] = 0$, with $\hat{H}$ the system Hamiltonian. We name this the reference gauge and refer to its vector potential as $\mathbf{A}_{\text{ref}}(\mathbf{r})$ and to its paramagnetic current density as $\mathbf{j}_{p_{\text{ref}}}(\mathbf{r})$. In this reference gauge the set $\{m\}$ corresponds to the eigenvalues of $\hat{L}_z$ and both equalities in the relation (11) hold. The set $\{m\}$ is then a constant of motion and in this gauge it represents the z component of the angular momentum.

We now focus on the generic gauge corresponding to a generic vector potential $\mathbf{A}(\mathbf{r})$. In this generic gauge, the first equality of Eq. (11) holds, but the second equality holds only if $\hat{L}_z$ is a constant of motion in this gauge. Here we consider the quantity

$$\tilde{\mathbf{j}}_p(\mathbf{r}) \equiv \mathbf{j}_p(\mathbf{r}) - \rho(\mathbf{r})\nabla\chi_{\text{ref}} \quad (17)$$

and the operator

$$\tilde{L}_z \equiv \sum_{i=1}^{N} [\mathbf{r} \times (\hat{\mathbf{p}} - \nabla\chi_{\text{ref}})]_z, \quad (18)$$

where $\nabla\chi_{\text{ref}}$ is defined by $\mathbf{A} = \mathbf{A}_{\text{ref}} - \nabla\chi_{\text{ref}}$. We note that $\tilde{\mathbf{j}}_p(\mathbf{r})$ is gauge invariant, as, from Eq. (14),

$$\tilde{\mathbf{j}}_p(\mathbf{r}) \equiv \mathbf{j}_{p_{\text{ref}}}(\mathbf{r}) \quad (19)$$

always. It follows that

$$\int [\mathbf{r} \times \tilde{\mathbf{j}}_p(\mathbf{r})]_z d\mathbf{r} = m \quad (20)$$

independently of the gauge. Furthermore, by using the definition (17), where $\rho(\mathbf{r}) = \int |\psi(\mathbf{r},\mathbf{r}_2\ldots\mathbf{r}_N)|^2 d\mathbf{r}_2\ldots d\mathbf{r}_N$, and the first equality of Eq. (11), which holds regardless of whether or not $\hat{L}_z$ is a constant of motion, we obtain

$$\int [\mathbf{r} \times \tilde{\mathbf{j}}_p(\mathbf{r})]_z d\mathbf{r} = \langle\psi|\hat{L}_z|\psi\rangle - \int [\mathbf{r} \times \rho(\mathbf{r})\nabla\chi_{\text{ref}}]_z d\mathbf{r}$$

$$= \langle\psi|\hat{L}_z|\psi\rangle - \langle\psi|(\mathbf{r} \times \nabla\chi_{\text{ref}})_z|\psi\rangle$$

$$= \langle\psi|\tilde{L}_z|\psi\rangle. \quad (21)$$

This demonstrates that Eq. (18) defines the operator associated to the conservation law (20) independently of the gauge. In particular, comparison of Eqs. (20) and (21) shows that indeed $\tilde{L}_z$ is the operator whose eigenvalues are $\{m\}$ independently

of the gauge.[2] Here $\tilde{L}_z$ reduces to $\hat{L}_z$ in the reference gauge and in all gauges where $\hat{L}_z$ is a constant of motion, as should be expected. This is because the limited set of gauges for which $[\hat{L}_z, \hat{H}] = 0$ holds, is the same within which both $\hat{L}_z$ and $[\mathbf{r} \times \mathbf{j}_p(\mathbf{r})]_z$ are unaffected by gauge transformations. These gauges correspond to vector potentials of the form

$$\mathbf{A}(\mathbf{r}) = [x\alpha + y\beta, y\alpha - x\beta, \gamma], \quad (22)$$

where α, β, and γ are all arbitrary functions of $(x^2 + y^2, z)$. These vector potentials are linked by gauge transformations of the form $\chi(x^2 + y^2, z)$. Demonstration of these statements is quite long and the details are given in Appendix B. Using the conservation law (20), we derive the metric

$$D_{\tilde{\mathbf{j}}_{p_\perp}}(\tilde{\mathbf{j}}_{p_1}, \tilde{\mathbf{j}}_{p_2}) = \int \left|\left\{\mathbf{r} \times [\tilde{\mathbf{j}}_{p_1}(\mathbf{r}) - \tilde{\mathbf{j}}_{p_2}(\mathbf{r})]\big|_z\right\}\right|d\mathbf{r} \quad (23)$$

for the gauge invariant current density $\tilde{\mathbf{j}}_p(\mathbf{r})$.

IV. METRIC ANALYSIS OF GROUND STATES FOR VARYING MAGNETIC FIELDS

In the presence of a magnetic field the metric spaces for ground-state wave functions, particle densities and paramagnetic current densities are characterized by a "band structure" [8]. This is significant as identification and characterization of ground-state properties is very important in several contexts but far from obvious. This "band structure" originates from the conservation law involving the paramagnetic current density $\mathbf{j}_p$. In $\mathbf{j}_p$ metric space, when considering variations in the scalar potential [8], the "band structure" is formed by spherical segments of allowed and forbidden distances on the concentric spheres, at least for the systems analyzed. The specific arc length of these segments varies depending on the radius $|m|$ of the sphere. Here we wish to investigate how this "band structure" responds to changes in the magnetic field.

A. Model systems

We focus on two atomiclike model systems with uniform, time-independent magnetic fields $\mathbf{B} = \omega_c c\hat{\mathbf{z}}$ applied, where c is the speed of light. Both systems consist of two electrons in harmonic confinement but with different electron-electron interactions. One system, known as the magnetic Hooke's atom, has a two-body Coulomb interaction [9,19], whereas in the other electrons interact via an inverse square interaction (ISI), the relative strength of which can be varied through an interaction parameter α [20]. The Hamiltonians for these systems are

$$\hat{H}_{HA} = \sum_{i=1}^{2}\left\{\frac{1}{2}\left[\hat{\mathbf{p}}_i + \frac{1}{c}\mathbf{A}(\mathbf{r}_i)\right]^2 + \frac{1}{2}\omega_0^2 r_i^2\right\} + \frac{1}{|\mathbf{r}_2 - \mathbf{r}_1|} \quad (24)$$

---

[2]We note that $\tilde{L}_z$ is related to the gauge invariant z component of the moment of mechanical momentum $\hat{K}_z = \hat{L}_z + [\mathbf{r} \times \mathbf{A}(\mathbf{r})]_z$ as $\tilde{L}_z = \hat{K}_z - (\mathbf{r} \times \mathbf{A}_{\text{ref}})_z$, but that $\hat{K}_z$ would not be a constant of motion in all gauges, that is, its eigenvalues are generally different from $\{m\}$. Likewise $\tilde{\mathbf{j}}_p$ does not coincide with the gauge-invariant total current density $\mathbf{j}(\mathbf{r}) = \mathbf{j}_p(\mathbf{r}) + \rho\mathbf{A}(\mathbf{r})$.

and

$$\hat{H}_{ISI} = \sum_{i=1}^{2}\left\{\frac{1}{2}\left[\hat{\mathbf{p}}_i + \frac{1}{c}\mathbf{A}(\mathbf{r}_i)\right]^2 + \frac{1}{2}\omega_0^2 r_i^2\right\} + \frac{\alpha}{(\mathbf{r}_1 - \mathbf{r}_2)^2}. \quad (25)$$

Here $\mathbf{A} = \frac{1}{2}(\mathbf{B} \times \mathbf{r})$ in the symmetric gauge, which is of the form of Eq. (22). Following Ref. [17], we neglect spin terms in the Hamiltonians to concentrate on the features of the orbital currents. For the ISI system, we can solve the time-independent Schrödinger equation exactly for all frequencies and values of m and α. However, for Hooke's atom, analytical solutions only exist for a discrete set of frequencies. In order to give us freedom over the frequencies we choose, we solve the Schrödinger equation with the method in Ref. [21], which allows us to numerically determine the solution with high precision for all frequencies.

We generate families of ground states by varying the magnetic field via the cyclotron frequency ω_c while holding the confinement frequency ω_0 and all other parameters in the Hamiltonian constant. For each ω_c value we calculate the wave function, particle density, and paramagnetic current density. Within each family, one value of ω_c (and hence m) is selected as a reference ($\omega_{c_{\text{ref}}}$ and m_{ref}, respectively), with the appropriate metrics used to find the distance between the physical functions at the reference and all of the other states in the family. We choose the reference so that most of the available distance range is explored for both increasing and decreasing ω_c.

Figure 2 shows that, for both of our systems, the value of m for which the energy is lowest decreases from zero through the negative integers as ω_c increases. Consequently, when studying ground states, we must consider states on different spheres in the paramagnetic current density metric space. We also note that there are "transition frequencies", i.e., values of ω_c where the energy is equal for two consecutive values of m. These are the crossings of the energy curves in Fig. 2. Therefore, when varying ω_c it is necessary to change the value of m at the transition frequencies in order to continue analyzing ground states. Additionally, when $m = 0$, $\mathbf{j}_p(\mathbf{r}) = 0$ for all $\mathbf{r}$. Hence, we take only negative values of m to ensure we consider ground states with nonzero paramagnetic current densities.

B. Ground states' band structure and relevance to current density-functional theory

An important research area where properties of ground states are central is DFT. This theory has produced widely used tools for realistic calculations of properties of many-body systems, such as band structures of metals and semiconductors, crystal structures of solids, and characterization of nanostructures [22,23]. Density-functional theory is founded upon the Hohenberg-Kohn (HK) theorem [24], which states that there is a one-to-one mapping between ground-state wave functions and ground-state particle densities. There are various forms of DFT that extend the application of the theory to a greater range of systems. Current-density-functional theory is the extension of standard DFT to include systems subject to external magnetic fields [17]. There is a HK-like theorem at the core of CDFT that states that a one-to-one mapping exists between the ground-state wave function ψ and, taken together, the particle density $\rho(\mathbf{r})$ and the paramagnetic current density
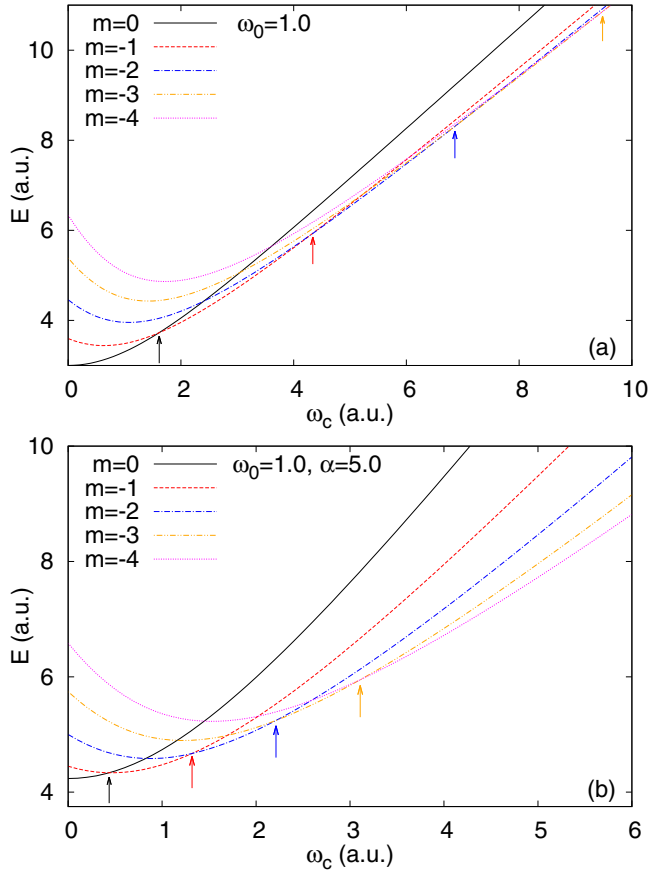
FIG. 2. (Color online) Energy plotted against the cyclotron frequency for several values of m for (a) Hooke's atom and (b) the ISI system. The confinement frequency and interaction strength are held constant. Arrows indicate where the value of m for the ground-state changes.

$\mathbf{j}_p(\mathbf{r})$ (the CDFT HK theorem) [17]. This additional complexity of the CDFT HK theorem with respect to the original HK theorem is due to the fact that systems with magnetic fields are characterized not only by a scalar potential (the external potential), but also by the vector potential connected to the magnetic field [17]. In Ref. [8] we started examining the CDFT HK mapping by looking at the effect of varying the scalar potential, i.e., the external confining potential; here we wish to complete this analysis by looking at the effect on the mapping of varying the vector potential, i.e., the magnetic field.

We start by comparing the distances between wave functions, their related particle densities, and their related paramagnetic current densities. Figure 3 shows plots of the relationships between the various distances considered, with each point referring to a particular value of ω_c. Let us consider first the plots of particle density distance against wave-function distance [Figs. 3(a)–3(d)]. As observed in Ref. [8], metric-space regions corresponding to ground states present a "band structure", where points associated with the same value of $|m|$ are grouped into distinct segments, i.e., bands. However, in contrast to the "band structure" observed in Ref. [8] [sketched in Fig. 4(a)], when varying the vector potential we obtain a series of "overlapping bands", where the minimum wave-function and minimum particle density distances for one value of $|m|$ are smaller than the maximum

distances for the previous value of $|m|$. This implies that there is an overlap between the projections of the bands on the metric-space sphere representing the densities, as sketched in Fig. 4(b) (similarly for the projection on the sphere representing the wave functions). Though overlapping, this "band structure" still results in discontinuities in the relationship between D_ρ and D_ψ when the value of m changes. Unlike when varying ω_0 [8], by varying the magnetic field we do not observe any forbidden distances, so we cannot identify forbidden regions for ground states by considering the particle density and wave-function metric spaces alone. In the range of distances explored here, nearby wave functions are mapped onto nearby particle densities and distant wave functions are mapped onto distant particle densities. However, in contrast to Ref. [8], the mapping is only piecewise linear: When acting on the vector potential, as ω_c is swept through each transition frequency, ground states and their particle densities abruptly revert to be closer to the reference state, while an almost linear mapping is maintained within two consecutive transition frequencies. The segments created in this way do not overlap, as, at each transition frequency, the ball related to the particle density and centered at the reference density shrinks proportionally more than the corresponding ball related to the wave function. Also, in contrast with Ref. [8], the two families of ground states corresponding to $|m| < |m_{\mathrm{ref}}|$ and $|m| > |m_{\mathrm{ref}}|$ describe distinct paths in metric space [e.g., compare Figs. 3(a) and 3(b)], with the size of the bands greater for $|m| < |m_{\mathrm{ref}}|$ compared to $|m| > |m_{\mathrm{ref}}|$. For all of these reasons the CDFT HK mapping between wave functions and related particle densities acquires added complexity when varying the vector potential compared to varying the scalar potential [compare Figs. 2(a) and 2(b) in Ref. [8] with Figs. 3(a)–3(d)].

In Figs. 3(e)–3(h) we consider paramagnetic current density distance against wave-function distance. Here we find once more an overlapping "band structure" for wave-function distances; however, a "band structure" with regions of allowed (bands) and forbidden (gaps) distances is observed for paramagnetic current density distances. In contrast with the one sketched in Fig. 4(a), in this case each band resides on a different sphere according to the value of $|m|$ (the radius of the sphere). Transition frequencies are points of discontinuity for both paramagnetic current density and wave-function distances. As for Figs. 3(a)–3(d), the curves for increasing and decreasing ω_c (and hence $|m|$) do not overlap, with larger bands for small values of $|m|$. Finally, Figs. 3(i)–3(l) present the plots of paramagnetic current density distance against particle density distance. These exhibit behavior similar to that in Figs. 3(e)–3(h).

The overlapping "band structures" observed in Fig. 3 demonstrate that mappings between some of the distances considered here are multivalued. This multivalued mapping does *not* represent a contradiction of the CDFT HK theorem as it is entirely possible to have distinct functions at the same distance away from a reference. In particular, in terms of the "onion-shell" geometry, all states situated at the same polar angle and on the same sphere will have the same distance from the reference state.

In Fig. 5 the wave-function and paramagnetic current density distances are plotted against ω_c for both systems,
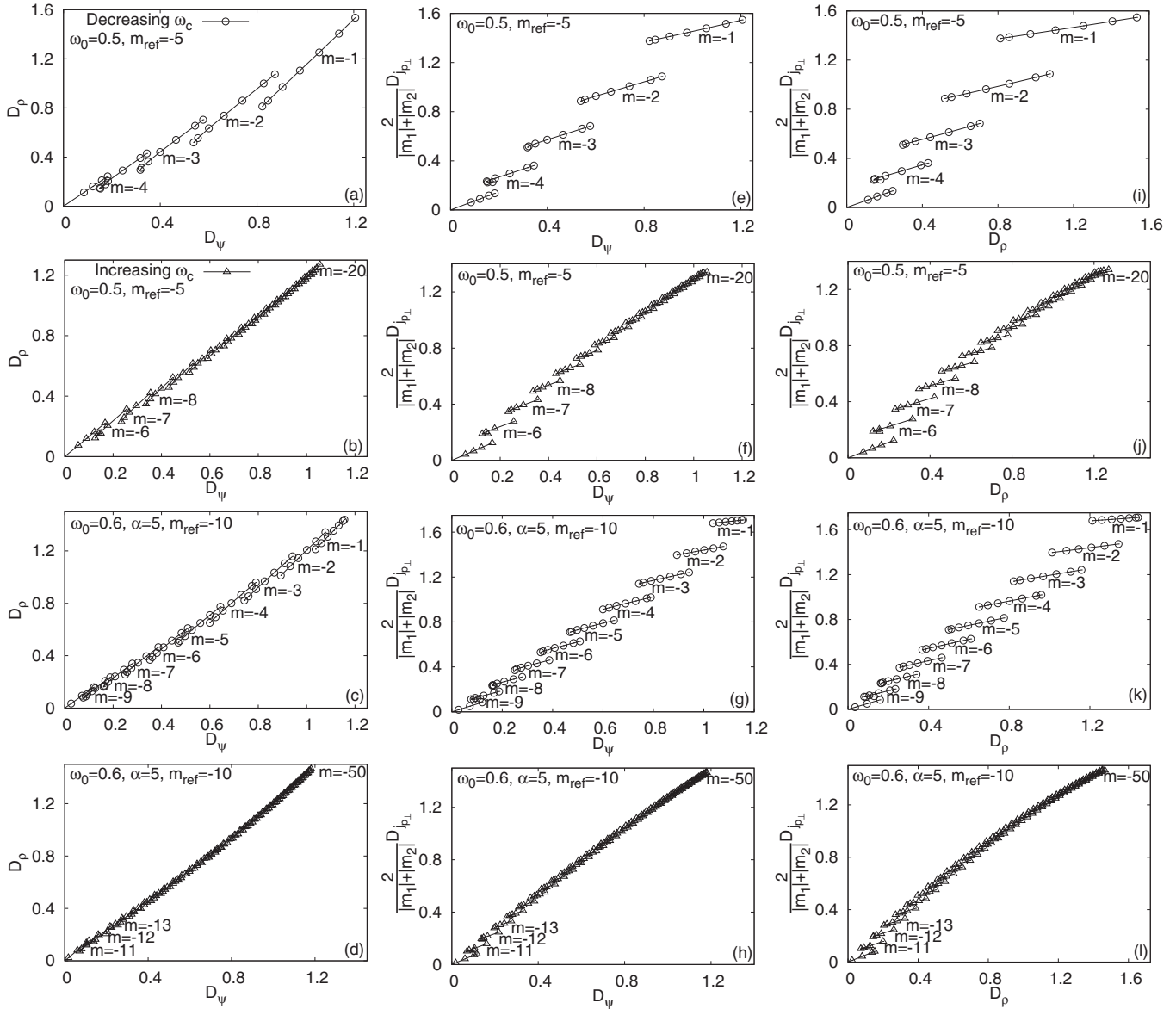
FIG. 3. Plots of distances for Hooke's atom with reference state $\omega_0 = 0.5$, $\omega_c = 5.238$, and $m_{\text{ref}} = -5$ (top two rows) and for the ISI system with reference state $\omega_0 = 0.6$, $\omega_c = 5.36$, $\alpha = 5$, and $m_{\text{ref}} = -10$ (bottom two rows): (a)–(d) particle density distance against wave-function distance, (e)–(h) paramagnetic current density distance against wave-function distance, and (i)–(l) paramagnetic current density distance against particle density distance. The reference frequency is taken halfway between the two transition frequencies related to m_{ref}.

enabling the "band structures" for individual functions to be analyzed. We note that, as observed in Fig. 3, there is a decrease in the wave-function distance at transitions [Figs. 5(a) and 5(b)], but an increase in the paramagnetic current density distance [Figs. 5(c) and 5(d)]. These features give rise to overlapping-band and band-gap structures, respectively. The other major feature is that, when varying ω_c, there is nonmonotonic behavior within bands corresponding to values of m close to m_{ref} (see insets). For both wave functions and paramagnetic current densities, we observe that immediately after each transition frequency, the distances initially decrease to a minimum for that particular band before increasing to the maximum for the band. This occurs at the transition frequency to the next band. This behavior is more pronounced for wave functions than for paramagnetic current densities. As stated,

the nonmonotonicity is not in contradiction with the HK-like theorem of CDFT, but shows a richer behavior with respect to what was observed in Ref. [8] when varying the scalar (confining) potential.

We point out that the "band structure" in metric space for paramagnetic current density is fundamentally different from the ones for particle density and wave function, as the former develops on different spheres, one band for each sphere, while the latter are within a single sphere where they may display overlapping-band or band-gap structures (see Fig. 4). All these band structures originate from the conservation law characterizing the paramagnetic current density and the features of the metric spaces for wave functions and particle densities are a direct consequence of the mapping of $\mathbf{j}_p(\mathbf{r})$ onto $\psi(\mathbf{r})$ and onto $\rho(\mathbf{r})$. In this sense the "band structure"
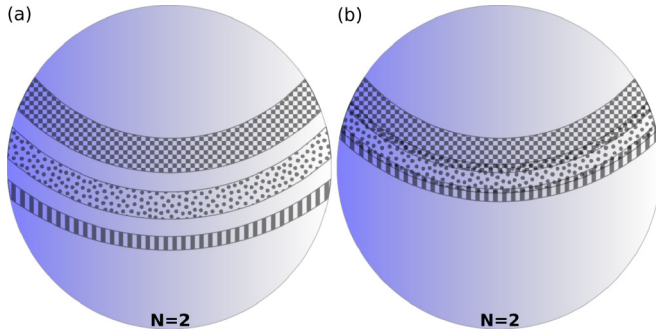
FIG. 4. (Color online) Sketches of "band structures" consisting of (a) "bands" and "gaps" and (b) "overlapping bands" in particle density metric space for three consecutive bands, where a different patterning corresponds to a different value of m. The reference state is at the north pole.

features of the metric spaces for wave functions and particle densities could be seen merely as the projections done by these mappings of the "band structure" characterizing the paramagnetic current density.

Finally, we wish to concentrate on the implications of our findings for CDFT. Current-density-functional theory requires that both ρ and $\mathbf{j}_p$ are taken together to ensure a one-to-one mapping to the wave function. The metric analysis allows us to provide evidence for an important aspect of this mapping, that is, to understand when the inclusion of $\mathbf{j}_p$ in the mapping becomes really crucial for the one-to-one correspondence to hold.

We present in Fig. 6 the ratio $D_{\mathbf{j}_{p_\perp}}/D_\rho$ against D_ψ for both Hooke's atom and the ISI system. From the data it is immediately clear that, in metric space, to a good level of approximation, $D_{\mathbf{j}_{p_\perp}} = \mathrm{const} \times D_\rho$ as long as $m = m_{\mathrm{ref}}$. This constant is the same for $\omega_c > \omega_{c_{\mathrm{ref}}}$ and $\omega_c < \omega_{c_{\mathrm{ref}}}$. These findings suggest that, at least for the systems at hand, as long as we remain on the same sphere in the paramagnetic current density metric space, $\mathbf{j}_p$ and ρ carry very similar information and the role of $\mathbf{j}_p$ in the core mapping of CDFT is secondary. The situation becomes very different for ground states with $m \neq m_{\mathrm{ref}}$. In this case the ratio $D_{\mathbf{j}_{p_\perp}}/D_\rho$ is far from constant and Fig. 6 clearly shows that the information contents of $\mathbf{j}_p$ and ρ are both necessary to define the state. Similar results are obtained when keeping the magnetic field fixed but varying the confinement ω_0 of the systems (not shown).

The characterization of this difference in the role of $\mathbf{j}_p$ and ρ in the CDFT core mapping constitutes one of the main results of the paper. To support it, we will analyze in the next section the behavior of states where m is kept equal to m_{ref} at all values of ω_c.

V. EXCITED STATES

Although an understanding of the ground state is important for studying systems subject to magnetic fields, it is often necessary to go beyond ground states, for example, when studying rapidly varying fields or spintronic devices that operate with excited states. With the metrics at hand, we investigate excited states and consider distances between
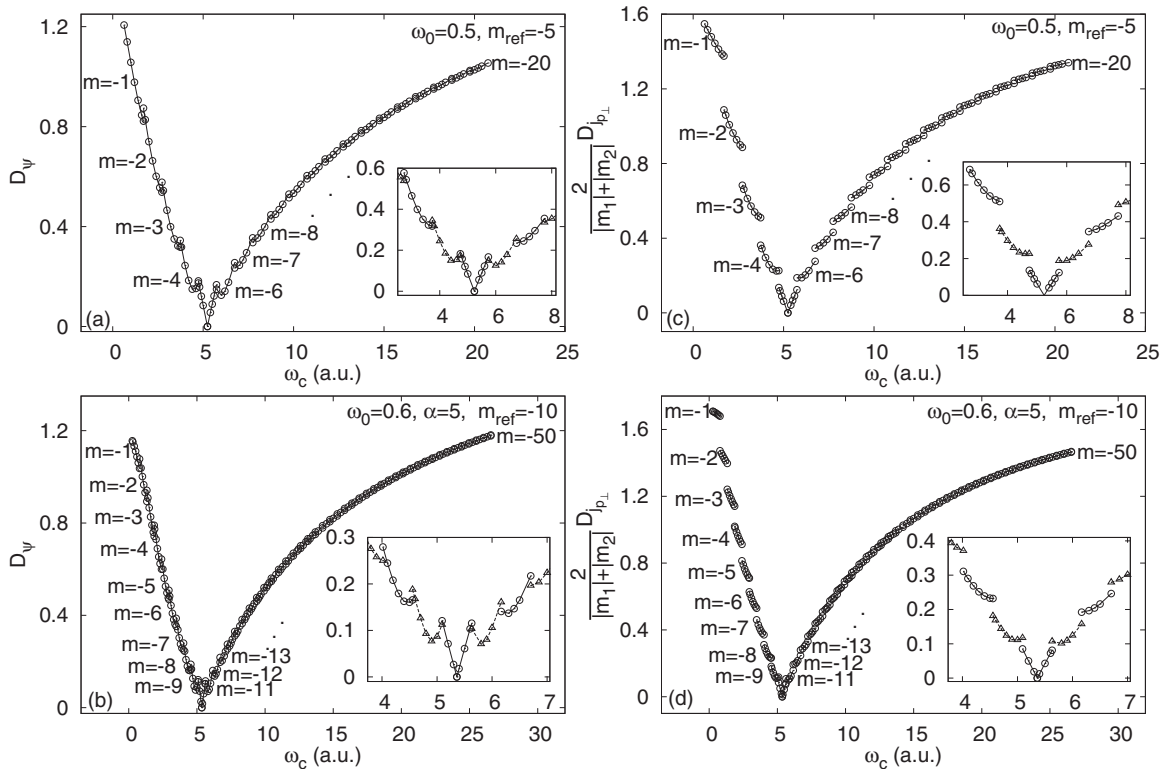

FIG. 5. For Hooke's atom (top) and the ISI system (bottom), (a) and (b) wave-function distance and (c) and (d) paramagnetic current density distance are plotted against ω_c. The behavior around the reference frequency is shown in each inset. The reference states are $\omega_0 = 0.5$, $\omega_{c_{\mathrm{ref}}} = 5.238$, and $m_{\mathrm{ref}} = -5$ for Hooke's atom and $\omega_0 = 0.6$, $\omega_{c_{\mathrm{ref}}} = 5.36$, $\alpha = 5$, and $m_{\mathrm{ref}} = -10$ for the ISI system.
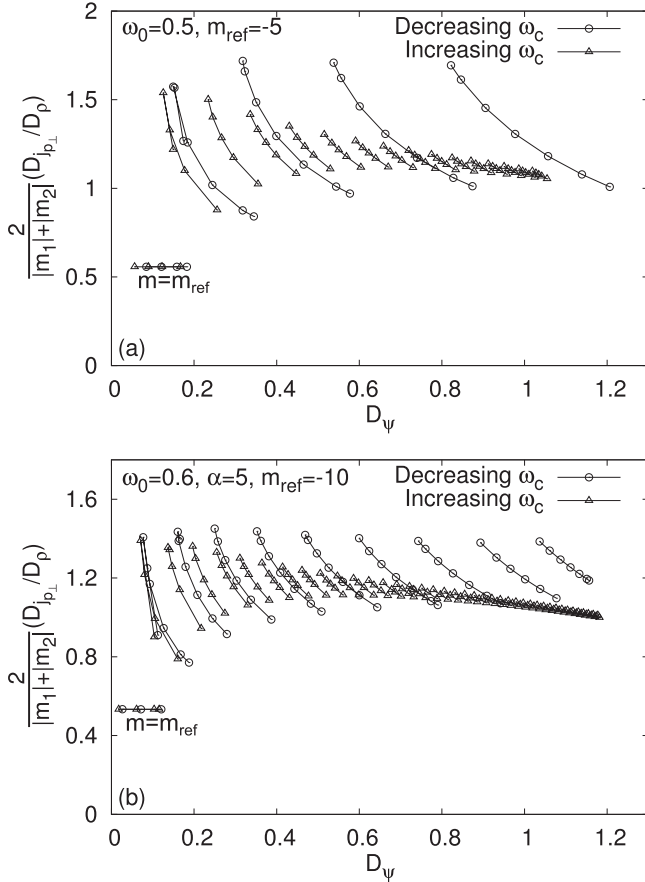
FIG. 6. Plots of the ratio of paramagnetic current density distance to particle density distance against wave-function distance for (a) Hooke's atom with reference state $\omega_0 = 0.5$, $\omega_{c_{ref}} = 5.238$, and $m_{ref} = -5$ and (b) the ISI system with reference state $\omega_0 = 0.6$, $\omega_{c_{ref}} = 5.36$, $\alpha = 5$, and $m_{ref} = -10$.

families of states corresponding to fixed values of m.[3] For each value of m we will construct a family of states by varying ω_c (ω_0 and α kept constant) and calculating the corresponding wave functions, particle densities, and paramagnetic current densities. As for ground states, we choose $m < 0$. With respect to Fig. 2, this corresponds to following single energy curves smoothly, i.e., without switching to a different curve at crossings, as done instead for the ground-state case. Each family of states will then lie on a particular sphere in the paramagnetic current density metric space. As the states considered are not necessarily ground states (see Fig. 2), there is no one-to-one mapping between the wave function and particle and paramagnetic current densities, but, these being fundamental quantities that characterize the system, we will still explore their relationships. Additionally, the study of these quantities allows us to corroborate the findings related to Fig. 6.

Figure 7 shows the relationship between each pair of distances for six different values of m. For any pair of distances here discussed, we find a monotonic relationship that is linear in the short- to intermediate-distance regime, before one of

the two functions rises more sharply to its maximum (see also Fig. 8). The mapping between the physical functions is such that nearby functions a (e.g., the wave functions) are mapped onto nearby functions b (e.g., the paramagnetic current densities) and distant functions a are mapped onto distant functions b. Crucially, as opposed to ground states, distances do not form any kind of metric-space "band structure", confirming the origin of band structures as the changes in m.

Looking at wave-function distances against particle density distances in Figs. 7(a) and 7(b) and contrasting with Figs. 3(a)–3(d), we observe that the curves for increasing and decreasing ω_c and all values of $|m|$ collapse onto one another. This hints at a universal behavior of the mapping between particle density and wave function when all the physical quantities describing the system remain on the same sphere in the related metric space while a physical parameter is smoothly changed.

When considering paramagnetic current density distance against wave-function distance in Figs. 7(c) and 7(d), although the curves for increasing and decreasing ω_c collapse onto one another, the curves for different values of m are distinct, particularly when $|m|$ is low. For lower values of $|m|$ the linear region extends across a larger range of distances. There is also a relatively small increase in the gradient at greater distances for low $|m|$. The curves in Figs. 7(c) and 7(d) all start and end at the same points. With the rescaling for $D_{\mathbf{j}_{p_\perp}}$ used in Fig. 7, the curves tend to a limiting curve with increasing values of $|m|$. In Fig. 8 we show the relationship between wave-function distance and paramagnetic current density distance for the ISI system without rescaling $D_{\mathbf{j}_{p_\perp}}$. Here the curves for each value of $|m|$ intersect only at the origin and each has a unique maximum of $2|m|$ for the paramagnetic current density distance. We observe that the gradient of the initial linear region increases with $|m|$. Figure 9 shows, for the ISI system, that the gradient in this region increases linearly with $|m|$, $D_{\mathbf{j}_{p_\perp}} \approx k|m|D_\psi$, with $0 \leqslant k \leqslant 1$, and is approximately equal for both decreasing and increasing ω_c. Similar results are obtained for Hooke's atom (not shown). These results imply that when rescaled as in Fig. 7, the initial slope of the curves will always be below $45°$, a result also observed in Ref. [5] for the case in which different spheres in the wave-function metric-space geometry were considered.

When considering paramagnetic current density distance against particle density distance [Figs. 7(e) and 7(f)] we see that, as for $D_{\mathbf{j}_{p_\perp}}$ vs D_ψ, with the rescaling of Fig. 7 there are distinct curves for each value of m that converge onto a single curve as $|m|$ increases. As opposed to $D_{\mathbf{j}_{p_\perp}}$ vs D_ψ, the extent of the linear behavior of these curves is increasing as $|m|$ increases.

The behavior of the curves observed in Fig. 7 reflects the "onion-shell" geometry. For wave functions and particle densities the sphere radius is associated with the number of particles in the system, which is fixed for the systems considered. Thus, regardless of the value of $|m|$, wave functions and particle densities always lie on the same sphere in their respective metric spaces. The fact that the related curves still superimpose for changing $|m|$ seems to imply that the value of $|m|$ has no relevant effect on the curves representing the relative change of ψ and ρ for changing parameters, at least as long as they remain on the same sphere. In paramagnetic

---

[3]The center-of-mass quantum number M is held constant at zero throughout this analysis.
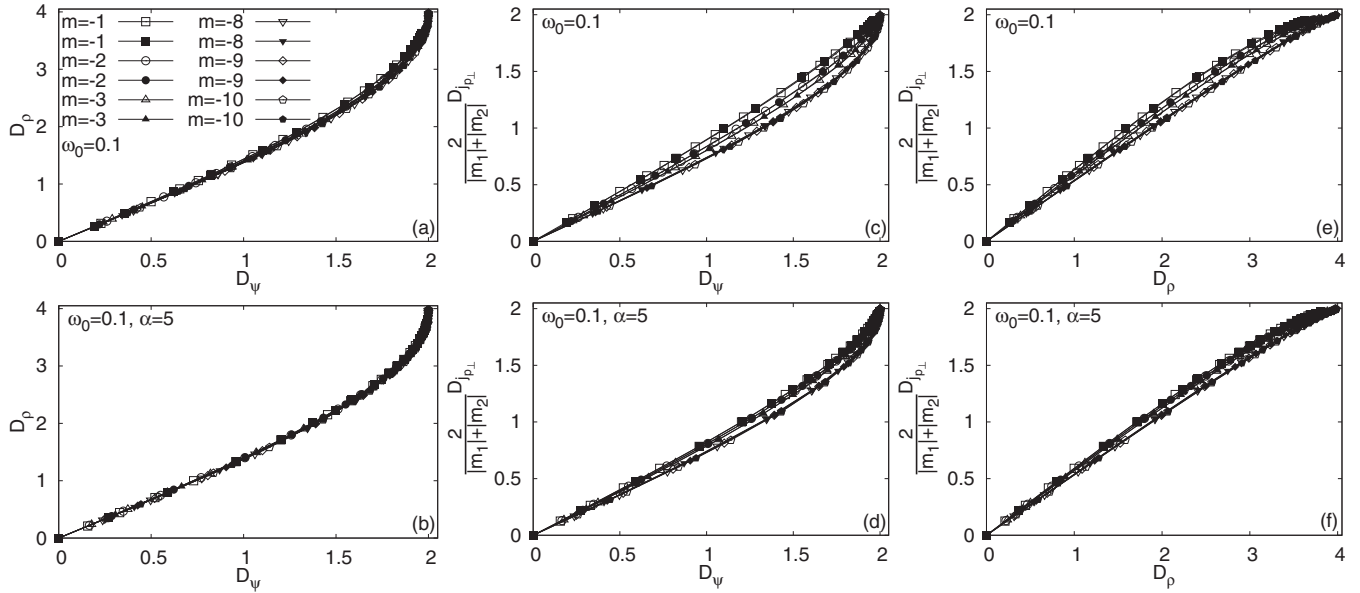
FIG. 7. Plots of (a) and (b) particle density distance against wave-function distance, (c) and (d) paramagnetic current density distance against wave-function distance, and (e) and (f) paramagnetic current density distance against particle density distance for $m = -1, -2, -3, -8, -9, -10$. The reference states for each value of m are $\omega_0 = 0.1$ and $\omega_{c_{ref}} = 30.0$ for Hooke's atom (top) and $\omega_0 = 0.1$, $\omega_{c_{ref}} = 5.0$, and $\alpha = 5$ for the ISI system (bottom). Closed symbols represent decreasing ω_c and open symbols represent increasing ω_c.

current density metric space, the spheres' radii are related to $|m|$, so paramagnetic current densities are on the surface of different spheres each time we consider a different value of $|m|$. As a result we see that the curves' shape is affected and they do not collapse onto each other. A similar universal behavior within each sphere and, by contrast, the breaking of this universality when different spheres were considered was also observed in Ref. [5], where different values of N, and hence different spheres, for both wave functions and particle densities were considered. This seems to suggest that different behavior for the mappings should be expected when curves on different spheres in the metric spaces are involved.

Finally, Fig. 10 combines all distances for each system in a single plot. Importantly, this figure shows that for small to medium wave-function distances $D_{j_{p\perp}}/D_\rho \sim$ const, where the constant depends on $|m|$, so this ratio is, to a good approximation, independent over variations of the wave function for relatively close wave functions. In this respect, for relatively close wave functions this suggests that the mappings between current density and wave function and between particle density and wave function are very similar, as long as the family of states follows the evolution of the
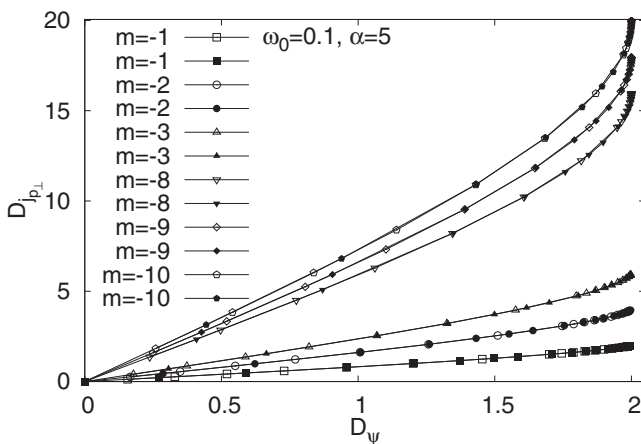

FIG. 8. Plot of paramagnetic current density distance against wave-function distance for $m = -1, -2, -3, -8, -9, -10$ for the ISI system. We take the state with $\omega_0 = 0.1$, $\omega_{c_{ref}} = 5.0$, and $\alpha = 5$ as a reference for each value of m and consider distances across the surface of each individual sphere.
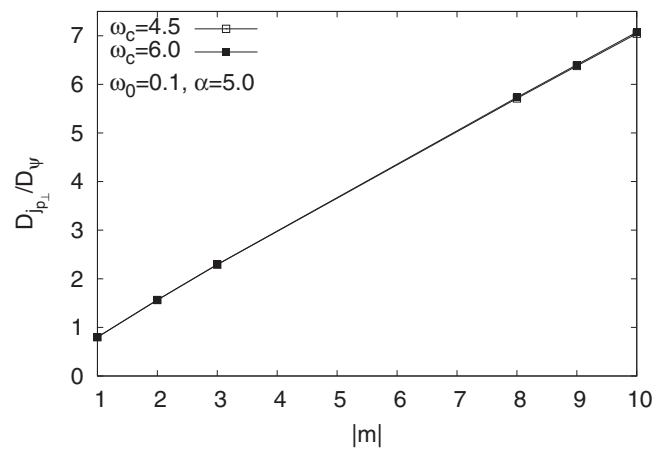

FIG. 9. Plot of the ratio of paramagnetic current density distance to wave-function distance against $|m|$ for the ISI system. The reference for each value of m is $\omega_0 = 0.1$, $\omega_{c_{ref}} = 5.0$, and $\alpha = 5$ and the gradient is taken at $\omega_c = 4.5$ for decreasing frequencies and $\omega_c = 6.0$ for increasing frequencies, i.e., the frequencies corresponding to the closest points to $\omega_{c_{ref}}$ for both decreasing and increasing ω_c in Fig. 8.
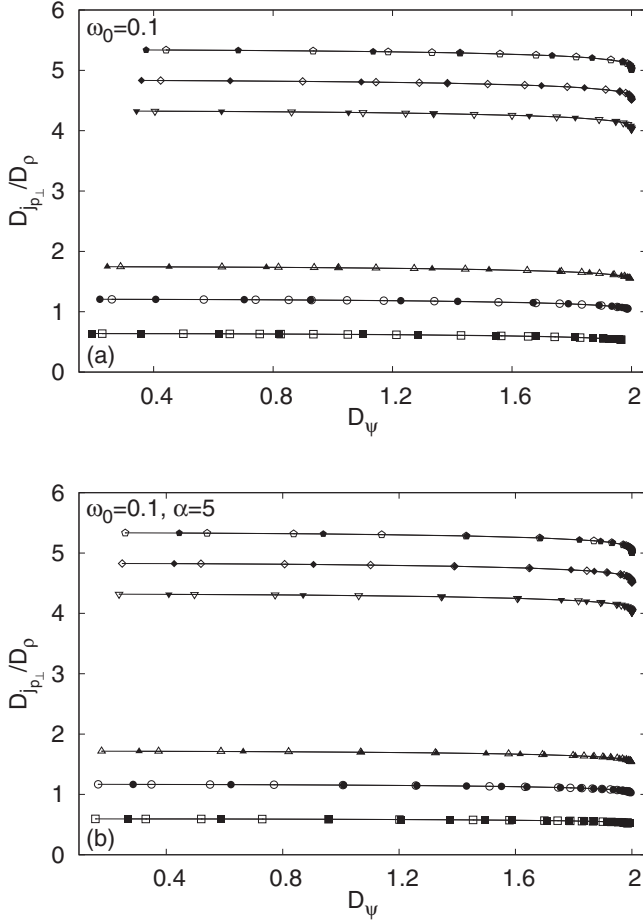
FIG. 10. Plots of the ratio of paramagnetic current density distance to particle density distance against wave-function distance for (a) Hooke's atom, with reference state $\omega_0 = 0.1$, $\omega_{c_{ref}} = 30.0$, and (b) the ISI system, with reference state $\omega_0 = 0.1$, $\omega_{c_{ref}} = 5.0$, and $\alpha = 5$. Closed symbols represent decreasing ω_c and open symbols represent increasing ω_c.

same energy eigenstate as driven by the varying parameter (see Fig. 2).

VI. CONCLUSION

The metric-space approach to quantum mechanics has enabled us to illustrate the role of the vector potential in systems subject to external magnetic fields, with particular reference to the fundamental concepts of CDFT. Importantly, we have also furthered the theoretical framework of the metric-space approach to quantum mechanics by discussing the key point of gauge invariance for the "natural" metrics proposed and in particular demonstrating the gauge-invariant metric for the paramagnetic current density, which is not a gauge-invariant quantity *per se*.

The presence of the vector potential in the Hamiltonian leads to the inclusion of the paramagnetic current density in the core mapping of CDFT. By considering the metric for the paramagnetic current density together with that for the particle density, we were able to investigate the relative contribution to this core mapping from each of these two

quantities, for the systems at hand. When m is held constant and paramagnetic current and particle densities belong to the same metric-space sphere as their reference state, we observed that the ratio $D_{\mathbf{j}_{p\perp}}/D_\rho$ is approximately constant, suggesting that ρ and $\mathbf{j}_p$ contribute similar information. However, this simple relation dramatically breaks down when considering states with $m \neq m_{\text{ref}}$ and hence states spanning different spheres in paramagnetic current density metric space. This suggests that the presence of $\mathbf{j}_p$ in the core mapping of CDFT becomes crucial in this case.

By varying the vector potential, we uncovered different aspects of the "band structure" in ground-state metric spaces, in particular the presence of overlapping bands, which enriches the band-gap structures already observed when varying the scalar potential. Our analysis suggests that, in general, the presence of bands in metric space can be expected when considering a family of states for which one of the fundamental physical functions spans more than one sphere in its metric space. For ground states, the onset of the "band structure" is the signature of energy levels' crossings obtained by varying a parameter in the Hamiltonian (the magnetic field in the present case).

We also applied the metric-space approach to quantum mechanics beyond ground states. When considering families of states characterized by fixed values of m, it was found that the mappings between wave functions, particle densities, and paramagnetic current densities are monotonic and almost linear, without "band structures", confirming that each band is characterized by a specific value of m. The curves D_ψ versus D_ρ superimpose for all values of m, but not so when $D_{\mathbf{j}_{p\perp}}$ is involved. This is consistent with the fact that a different m represents different spheres in the "onion-shell" geometry related to $\mathbf{j}_p$.

Finally, when considering the ratio $D_{\mathbf{j}_{p\perp}}/D_\rho$ for these fixed-m families, the relationship $D_{\mathbf{j}_{p\perp}}/D_\rho \approx \text{const}$ was observed to persist up to intermediate distances and for all of the values of m that were explored. At least for the systems at hand, this suggests that, within the same sphere and up to quite different states, particle density and wave function still suffice to contribute most of the information on the physical system.

APPENDIX A: GAUGE INVARIANCE FOR THE WAVE-FUNCTION METRIC

Gauge transformations affect wave functions by introducing a constant global phase factor [see Eq. (13)]. Wave functions differing by this phase factor describe the same physics; in fact, the solutions of the Schrödinger equation are only defined up to a global phase factor. To have physically meaningful metrics, it is therefore important to

define equivalence classes such that the metric assigns zero distance to wave functions differing only by a *global* phase factor.

An equivalence class for an element $x \in X$ is defined as [25]

$$[x] = \{x' \in X : x \sim x'\}, \tag{A1}$$

where $\sim$ is the equivalence relation. Each element of the set X belongs to a single equivalence class [25].

In order to account for an equivalence relation between elements $x \sim x'$, we follow a general procedure for introducing equivalence relations into a metric space (X, D). We define the function [26]

$$D_R(x,y) = \inf \left\{ \sum_{i=1}^{k} D(p_i, q_i) : p_1 = x, q_k = y, k \in \mathbb{N} \right\}, \tag{A2}$$

where the infimum is taken over all choices of $\{p_i\}$ and $\{q_i\}$ such that $p_{i+1} \sim q_i$. This implies that if $x \sim y$, $D_R(x,y) = D(x,x) + D(y,y) = 0$ even if $D(x,y) \neq 0$ [26]. This function is a semimetric (or pseudometric) on the set X, known as the quotient semimetric. A semimetric is a distance function that obeys all of the axioms of a metric except that it allows zero distance between nonidentical elements as well as identical ones.

For wave functions, the metric derived from the conservation law before accounting for the equivalence of wave functions differing by a global phase is [5,27]

$$\tilde{D}_\psi(\psi_1, \psi_2) = \left[\int |\psi_1 - \psi_2|^2 d\mathbf{r}_1 \cdots d\mathbf{r}_N \right]^{1/2}. \tag{A3}$$

For this in general we have that $\tilde{D}_\psi(\psi, e^{i\phi}\psi) \neq 0$. If in Eq. (A2) we take $k = 2$, we find

$$D_\psi(\psi_1, \psi_2) = \inf\{\tilde{D}_\psi(\psi_1, \psi') + \tilde{D}_\psi(\psi_2, \psi_2)\}$$
$$= \inf\{\tilde{D}_\psi(\psi_1, \psi')\},$$

where $\psi' = e^{i\phi}\psi_2 \sim \psi_2$ and we have used the positivity axiom of the metric. The choice of ψ' that will minimize the value of the semimetric is determined by the phase factor, hence

$$D_\psi(\psi_1, \psi_2) = \min_{\phi} \{\tilde{D}_\psi(\psi_1, e^{i\phi}\psi_2)\}. \tag{A4}$$

With this semimetric space $(\{\psi\}, D_\psi)$, we can recover a metric space in a natural way, by "gluing" equivalent elements to form a set of equivalence classes. By considering the set of equivalence classes, rather than the set of all wave functions, all wave functions differing only by a global phase factor are identified with one another. Thus, for wave functions, the set of equivalent wave functions with D_ψ is a metric space, with the metric defined between each of the equivalence classes, as required [25]. The metric D_ψ defined from Eq. (A4) is the same as the metric defined in Refs. [5,27] and can be expressed in the form of Eq. (8).

APPENDIX B: DETERMINING THE GAUGES WHERE L_z IS A CONSTANT OF MOTION

In order to be a constant of motion, the z component of the angular momentum $\hat{L}_z = -i[\mathbf{r} \times \nabla]_z$ must commute with the Hamiltonian. Given that a vector potential is present, we consider the Pauli Hamiltonian

$$\hat{H} = -\frac{1}{2}\nabla^2 - \frac{i}{2}(\mathbf{A} \cdot \nabla + \nabla \cdot \mathbf{A}) + \frac{1}{2}A^2 + V(\mathbf{r}), \tag{B1}$$

with $V(\mathbf{r})$ such that $[V(\mathbf{r}), \hat{L}_z] = 0$. The Hamiltonian (B1) does not necessarily commute with $\hat{L}_z$ for a particular $\mathbf{A}(\mathbf{r})$, because $\hat{L}_z$ is gauge variant. For instance, $\hat{L}_z$ commutes with the Hamiltonian (B1) in the symmetric gauge $\mathbf{A} = [y, -x, 0]$ and does not commute with it in the Landau gauge $\mathbf{A} = [0, -x, 0]$. We wish to determine the general set of vector potentials where $[\hat{H}, \hat{L}_z] = 0$.[4]

1. Simplifying the commutator

The commutator we wish to evaluate is

$$[\hat{H}, \hat{L}_z]\psi = -i\left[\mathbf{A} \cdot \nabla\left(x\frac{\partial\psi}{\partial y}\right) - \mathbf{A} \cdot \nabla\left(y\frac{\partial\psi}{\partial x}\right) \right.$$
$$- x\frac{\partial}{\partial y}(\mathbf{A} \cdot \nabla\psi) + y\frac{\partial}{\partial x}(\mathbf{A} \cdot \nabla\psi) + \nabla \cdot \left(\mathbf{A}x\frac{\partial\psi}{\partial y}\right)$$
$$- \nabla \cdot \left(\mathbf{A}y\frac{\partial\psi}{\partial x}\right) - x\frac{\partial}{\partial y}\nabla \cdot (\mathbf{A}\psi) + y\frac{\partial}{\partial x}\nabla \cdot (\mathbf{A}\psi) \right]$$
$$+ A^2 x\frac{\partial\psi}{\partial y} - A^2 y\frac{\partial\psi}{\partial x} - x\frac{\partial}{\partial y}(A^2\psi) + y\frac{\partial}{\partial x}(A^2\psi), \tag{B2}$$

where we have used that $[-\frac{1}{2}\nabla^2 + V(\mathbf{r}), \hat{L}_z] = 0$. We wish to impose the condition $[\hat{H}, \hat{L}_z] = 0$ and then solve the commutator to obtain the vector potential $\mathbf{A}(\mathbf{r})$. After performing the vector operations and simplifying, Eq. (B2) reduces to

$$-i\left[\left(2A_x\frac{\partial\psi}{\partial y} - 2A_y\frac{\partial\psi}{\partial x}\right) \right.$$
$$- 2x\left(\frac{\partial\psi}{\partial x}\frac{\partial A_x}{\partial y} + \frac{\partial\psi}{\partial y}\frac{\partial A_y}{\partial y} + \frac{\partial\psi}{\partial z}\frac{\partial A_z}{\partial y}\right)$$
$$+ 2y\left(\frac{\partial\psi}{\partial x}\frac{\partial A_x}{\partial x} + \frac{\partial\psi}{\partial y}\frac{\partial A_y}{\partial x} + \frac{\partial\psi}{\partial z}\frac{\partial A_z}{\partial x}\right)$$
$$- x\psi\frac{\partial}{\partial y}\left(\frac{\partial A_x}{\partial x} + \frac{\partial A_y}{\partial y} + \frac{\partial A_z}{\partial z}\right)$$
$$+ y\psi\frac{\partial}{\partial x}\left(\frac{\partial A_x}{\partial x} + \frac{\partial A_y}{\partial y} + \frac{\partial A_z}{\partial z}\right) \right]$$
$$- x\psi\frac{\partial A^2}{\partial y} + y\psi\frac{\partial A^2}{\partial x} = 0. \tag{B3}$$

In order to progress with the solution of this equation, we first consider the case where $\psi, \frac{\partial\psi}{\partial x}, \frac{\partial\psi}{\partial y}$, and $\frac{\partial\psi}{\partial z}$ are all independent of each other. This choice allows us to decompose Eq. (B3) into a set of simultaneous equations, which we can then solve. The solution of these equations will provide properties of the general set of vector potentials where $[\hat{H}, \hat{L}_z] = 0$. Using these properties, we will then solve Eq. (B3) for $\mathbf{A}(\mathbf{r})$ using a general wave function.

----

[4]In the case where we have many-body interactions, we only consider the case $[U(\mathbf{r}_i, \mathbf{r}_j), \hat{L}_z] = 0$, as is the case for the Coulomb interaction.

With our choice of trial wave function, we write the set of simultaneous equations

$$ix\frac{\partial}{\partial y}\left(\frac{\partial A_x}{\partial x}+\frac{\partial A_y}{\partial y}+\frac{\partial A_z}{\partial z}\right)-x\frac{\partial A^2}{\partial y}$$

$$-\,iy\frac{\partial}{\partial x}\left(\frac{\partial A_x}{\partial x}+\frac{\partial A_y}{\partial y}+\frac{\partial A_z}{\partial z}\right)+y\frac{\partial A^2}{\partial x}=0, \quad\text{(B4)}$$

$$A_y+x\frac{\partial A_x}{\partial y}-y\frac{\partial A_x}{\partial x}=0, \quad\text{(B5)}$$

$$A_x-x\frac{\partial A_y}{\partial y}+y\frac{\partial A_y}{\partial x}=0, \quad\text{(B6)}$$

$$y\frac{\partial A_z}{\partial x}-x\frac{\partial A_z}{\partial y}=0. \quad\text{(B7)}$$

We concentrate first on Eqs. (B5)–(B7), a set of three equations for the three unknowns A_x, A_y, and A_z. Firstly, we consider Eq. (B7): In order to solve this partial differential equation (PDE), we use the method of characteristics [28].

The method of characteristics requires the visualization of Eq. (B7) in four-dimensional coordinates (x,y,z,u). By considering the solution surface $u = A_z(x,y,z)$, we can write

$$A_z(x,y,z)-u = 0.$$

For any surface S a normal vector to the surface is given by ∇S. Thus, the vector $[\frac{\partial A_z}{\partial x},\frac{\partial A_z}{\partial y},\frac{\partial A_z}{\partial z},-1]$ is normal to the solution surface. We now write the PDE (B7) as a scalar product

$$[y,-x,0,0]\cdot\left[\frac{\partial A_z}{\partial x},\frac{\partial A_z}{\partial y},\frac{\partial A_z}{\partial z},-1\right]=0.$$

Since the scalar product of these two vectors is zero, they must be orthogonal. Given also that the vector $[\frac{\partial A_z}{\partial x},\frac{\partial A_z}{\partial y},\frac{\partial A_z}{\partial z},-1]$ is normal to the surface, this tells us that the vector field $[y,-x,0,0]$ is tangent to the surface at every point, providing a geometrical interpretation of the PDE. Thus, any curve within the surface $A_z(x,y,z)-u=0$ that has the vector $[y,-x,0,0]$ as a tangent at every point must lie entirely within the surface. Such curves are called characteristic curves [28]. Any curve can be described by a parameter t and the tangent of such a curve $\mathbf{r}(t)$ is given by the derivative with respect to this parameter $\mathbf{r}'(t)$. Therefore, the tangent of a characteristic curve $\mathbf{r}(t)=[x(t),y(t),z(t),A_z(t)]$ is given by the vector

$$\mathbf{r}'(t)=\left[\frac{dx}{dt},\frac{dy}{dt},\frac{dz}{dt},\frac{dA_z}{dt}\right].$$

This vector is therefore proportional to the tangent vector $[y,-x,0,0]$ for this characteristic curve, allowing us to construct the equations

$$\frac{dx}{dt}=y, \quad\text{(B8)}$$

$$\frac{dy}{dt}=-x, \quad\text{(B9)}$$

$$\frac{dz}{dt}=0, \quad\text{(B10)}$$

$$\frac{dA_z}{dt}=0. \quad\text{(B11)}$$

These are the characteristic equations of the PDE (B7).

Solving this set of ordinary differential equations (ODEs) yields the solution of the original PDE (B7), since

$$\frac{dA_z}{dt}=\frac{dx}{dt}\frac{\partial A_z}{\partial x}+\frac{dy}{dt}\frac{\partial A_z}{\partial y}+\frac{dz}{dt}\frac{\partial A_z}{\partial z}$$

$$=y\frac{\partial A_z}{\partial x}-x\frac{\partial A_z}{\partial y}=0.$$

By eliminating the parameter t in Eqs. (B8)–(B11), we can reduce the set of ODEs to three equations

$$\frac{dy}{dx}=-\frac{x}{y}, \quad\text{(B12)}$$

$$\frac{dz}{dx}=0, \quad\text{(B13)}$$

$$\frac{dA_z}{dx}=0. \quad\text{(B14)}$$

We now note that the constant of integration in Eq. (B14) has a functional dependence on the solutions to Eqs. (B12) and (B13). This is because the ODEs are solved along characteristic curves: The constants of integration are constant along a particular characteristic, but can vary between characteristics. The solutions to Eqs. (B12) and (B13) are

$$x^2+y^2=a,\quad z=b, \quad\text{(B15)}$$

respectively, where a and b are the constants of integration. Thus, the solution for A_z is

$$A_z=\gamma(x^2+y^2,z), \quad\text{(B16)}$$

where γ is an arbitrary function.

2. Solving the simultaneous equations

We will now solve Eqs. (B5) and (B6) simultaneously. First, we differentiate Eq. (B5) with respect to both x and y, which gives

$$\frac{\partial A_y}{\partial x}+\frac{\partial A_x}{\partial y}+x\frac{\partial^2 A_x}{\partial x\partial y}-y\frac{\partial^2 A_x}{\partial x^2}=0, \quad\text{(B17)}$$

$$\frac{\partial A_y}{\partial y}+x\frac{\partial^2 A_x}{\partial y^2}-\frac{\partial A_x}{\partial x}-y\frac{\partial^2 A_x}{\partial x\partial y}=0, \quad\text{(B18)}$$

respectively. We substitute these expressions for $\frac{\partial A_y}{\partial x}$ and $\frac{\partial A_y}{\partial y}$ into Eq. (B6) and obtain

$$A_x-x\left(-x\frac{\partial^2 A_x}{\partial y^2}+\frac{\partial A_x}{\partial x}+y\frac{\partial^2 A_x}{\partial x\partial y}\right)$$

$$+\,y\left(-\frac{\partial A_x}{\partial y}-x\frac{\partial^2 A_x}{\partial x\partial y}+y\frac{\partial^2 A_x}{\partial x^2}\right)=0,$$

$$y^2\frac{\partial^2 A_x}{\partial x^2}-2xy\frac{\partial^2 A_x}{\partial x\partial y}+x^2\frac{\partial^2 A_x}{\partial y^2}-x\frac{\partial A_x}{\partial x}-y\frac{\partial A_x}{\partial y}+A_x=0. \quad\text{(B19)}$$

We now have an equation containing only the unknown A_x that we can solve.

We begin to solve this equation by using the method of characteristics. For second-order PDEs, it is first necessary to determine the type of the PDE, either hyperbolic, parabolic, or elliptic. This is done by calculating the discriminant b^2-4ac,

where a, b, and c are the coefficients of $\frac{\partial^2 A_x}{\partial x^2}$, $\frac{\partial^2 A_x}{\partial x \partial y}$, and $\frac{\partial^2 A_x}{\partial y^2}$, respectively. This will then allow us to perform an appropriate change of variables from (x,y,z) to (ξ,η,z), where ξ and η are the characteristics [29]. The discriminant is

$$b^2 - 4ac = 4x^2 y^2 - 4x^2 y^2 = 0. \qquad (B20)$$

Therefore, the characteristic equation is parabolic and has one repeated solution, which we take for ξ. The characteristic equation is the ODE [29]

$$y^2 \left(\frac{dy}{dx} \right)^2 - 2xy \frac{dy}{dx} + x^2 = 0; \qquad (B21)$$

solving for $\frac{dy}{dx}$ gives

$$\frac{dy}{dx} = -\frac{x}{y}.$$

Hence, from Eq. (B15) we know that the first characteristic is $\xi = a = x^2 + y^2$. Since there is only one root of the characteristic equation, we have complete freedom in the choice for η, provided that it is not the same as ξ. Given that we know that the symmetric gauge satisfies the commutator $[\hat{H}, \hat{L}_z] = 0$ and, specifically, that $A_x = y$ is a solution for Eq. (B19), we choose $\eta = y$. By using the chain rule, we find the derivatives in Eq. (B19),

$$\frac{\partial A_x}{\partial x} = 2x \frac{\partial A_x}{\partial \xi},$$

$$\frac{\partial A_x}{\partial y} = 2y \frac{\partial A_x}{\partial \xi} + \frac{\partial A_x}{\partial \eta},$$

$$\frac{\partial^2 A_x}{\partial x^2} = 4x^2 \frac{\partial^2 A_x}{\partial \xi^2} + 2 \frac{\partial A_x}{\partial \xi},$$

$$\frac{\partial^2 A_x}{\partial y^2} = 4y^2 \frac{\partial^2 A_x}{\partial \xi^2} + 4y \frac{\partial^2 A_x}{\partial \xi \partial \eta} + \frac{\partial^2 A_x}{\partial \eta^2} + 2 \frac{\partial A_x}{\partial \xi},$$

$$\frac{\partial^2 A_x}{\partial x \partial y} = 4xy \frac{\partial^2 A_x}{\partial \xi^2} + 2x \frac{\partial^2 A_x}{\partial \xi \partial \eta}.$$

Substituting into Eq. (B19) and simplifying, we get

$$x^2 \frac{\partial^2 A_x}{\partial \eta^2} - y \frac{\partial A_x}{\partial \eta} + A_x = 0$$

and completing the change of variables gives

$$(\xi - \eta^2) \frac{\partial^2 A_x}{\partial \eta^2} - \eta \frac{\partial A_x}{\partial \eta} + A_x = 0. \qquad (B22)$$

The next step of the solution is to perform a reduction of order through the use of the known solution $A_x = \eta$ [29]. The reduction used is

$$A_x = u\eta, \quad \frac{\partial A_x}{\partial \eta} = \eta \frac{\partial u}{\partial \eta} + u, \quad \frac{\partial^2 A_x}{\partial \eta^2} = \eta \frac{\partial^2 u}{\partial \eta^2} + 2 \frac{\partial u}{\partial \eta},$$

which we substitute into Eq. (B22) to give

$$\eta(\xi - \eta^2) \frac{\partial^2 u}{\partial \eta^2} + 2(\xi - \eta^2) \frac{\partial u}{\partial \eta} - \eta^2 \frac{\partial u}{\partial \eta} - u\eta + u\eta = 0,$$

$$\eta(\xi - \eta^2) \frac{\partial^2 u}{\partial \eta^2} + (2\xi - 3\eta^2) \frac{\partial u}{\partial \eta} = 0.$$

We now make the substitution $v = \frac{\partial u}{\partial \eta}$,

$$\eta(\xi - \eta^2) \frac{\partial v}{\partial \eta} + (2\xi - 3\eta^2)v = 0. \qquad (B23)$$

This equation can now be solved separably,

$$\int \frac{1}{v} dv = \int \left[\frac{3\eta^2 - 2\xi}{\eta(\xi - \eta^2)} \right] d\eta.$$

We decompose the denominator through the use of partial fractions, giving

$$\int \frac{1}{v} dv = -\int \frac{2}{\eta} d\eta + \int \frac{\eta}{\xi - \eta^2} d\eta,$$

from which we get

$$\ln v = -2 \ln \eta - \frac{1}{2} \ln \left| \xi - \eta^2 \right| + \ln \left[\alpha(\xi,z) \right],$$

$$v = \frac{\alpha(\xi,z)}{\eta^2 |\xi - \eta^2|^{1/2}},$$

where α is an arbitrary function and we note that $\xi - \eta^2 = x^2 + y^2 - y^2 = x^2 > 0$, hence $\xi - \eta^2$ is always positive.

Now that we have a solution to Eq. (B23), we must reverse our substitutions to get a solution for A_x. First, we integrate v to get u,

$$u = \alpha(\xi,z) \int \frac{1}{\eta^2 (\xi - \eta^2)^{1/2}} d\eta. \qquad (B24)$$

From standard integrals [30], we get

$$u = -\frac{\alpha(\xi,z)}{\xi \eta} (\xi - \eta^2)^{1/2} + \beta(\xi,z),$$

where β is another arbitrary function. Next we write $A_x = u\eta$, obtaining

$$A_x = \alpha(\xi,z)(\xi - \eta^2)^{1/2} + \eta \beta(\xi,z), \qquad (B25)$$

where we absorb the factor of $-\frac{1}{\xi}$ into α. Finally, we substitute back from (ξ,η,z) to (x,y,z),

$$A_x = \alpha(x^2 + y^2, z)(x^2 + y^2 - y^2)^{1/2} + y\beta(x^2 + y^2, z)$$

$$= x\alpha(x^2 + y^2, z) + y\beta(x^2 + y^2, z), \qquad (B26)$$

to give the solution for A_x. We find A_y from Eq. (B5),

$$A_y = y \frac{\partial A_x}{\partial x} - x \frac{\partial A_x}{\partial y}$$

$$= y[\alpha(x^2 + y^2, z) + 2x^2 \alpha'(x^2 + y^2, z) + 2xy\beta'(x^2 + y^2, z)] - x[2xy\alpha'(x^2 + y^2, z) + \beta(x^2 + y^2, z) + 2y^2\beta'(x^2 + y^2, z)]$$

$$= y\alpha(x^2 + y^2, z) - x\beta(x^2 + y^2, z),$$

giving us solutions for all three components. We will now verify that the solutions for A_x, A_y, and A_z satisfy the remaining equation (B4),

$$ix\frac{\partial}{\partial y}\left(\frac{\partial A_x}{\partial x} + \frac{\partial A_y}{\partial y} + \frac{\partial A_z}{\partial z}\right) - x\frac{\partial A^2}{\partial y} - iy\frac{\partial}{\partial x}\left(\frac{\partial A_x}{\partial x} + \frac{\partial A_y}{\partial y} + \frac{\partial A_z}{\partial z}\right) + y\frac{\partial A^2}{\partial x}$$

$$= ix\frac{\partial}{\partial y}\left(2\alpha + 2x^2\alpha' + 2xy\beta' + 2y^2\alpha' - 2xy\beta' + \frac{\partial\gamma}{\partial z}\right) - iy\frac{\partial}{\partial x}\left(2\alpha + 2x^2\alpha' + 2xy\beta' + 2y^2\alpha' - 2xy\beta' + \frac{\partial\gamma}{\partial z}\right)$$

$$- x(4x^2y\alpha\alpha' + 2y\beta^2 + 4y^3\beta\beta' + 2y\alpha^2 + 4y^3\alpha\alpha' + 4x^2y\beta\beta' + 4y\gamma\gamma')$$

$$+ y(2x\alpha^2 + 4x^3\alpha\alpha' + 4xy^2\beta\beta' + 4xy^2\alpha\alpha' + 2x\beta^2 + 4x^3\beta\beta' + 4x\gamma\gamma')$$

$$= i\left(4xy\alpha' + 4x^3y\alpha'' + 4xy\alpha' + 4xy^3\alpha'' + 2xy\frac{\partial\gamma'}{\partial z} - 4xy\alpha' - 4xy\alpha' - 4x^3y\alpha'' - 4xy^3\alpha'' - 2xy\frac{\partial\gamma'}{\partial z}\right)$$

$$= 0,$$

where a prime denotes differentiation with respect to $(x^2 + y^2)$. Therefore, the form of the vector potential required for $[\hat{H},\hat{L}_z] = 0$ is

$$\mathbf{A} = [x\alpha(x^2 + y^2,z) + y\beta(x^2 + y^2,z), y\alpha(x^2 + y^2,z) - x\beta(x^2 + y^2,z), \gamma(x^2 + y^2,z)]. \tag{B27}$$

This form of the vector potential satisfies the condition $[\hat{H},\hat{L}_z] = 0$ for wave functions with $\frac{\partial\psi}{\partial x}$, $\frac{\partial\psi}{\partial y}$, and $\frac{\partial\psi}{\partial z}$ all independent of each other. Clearly, vector potentials that are not of the form of Eq. (B27) do not satisfy the condition. However, in order to ensure that vector potentials of this form satisfy this condition for an arbitrary wave function, we use the properties of the vector potentials to solve the original commutator (B3) for an arbitrary wave function. This gives

$$[\hat{H},\hat{L}_z]\psi = -i\left\{2(x\alpha + y\beta)\frac{\partial\psi}{\partial y} - 2(y\alpha - x\beta)\frac{\partial\psi}{\partial x} - 2x\left[(2xy\alpha' + \beta + 2y^2\beta')\frac{\partial\psi}{\partial x} + (\alpha + 2y^2\alpha' - 2xy\beta')\frac{\partial\psi}{\partial y} + 2y\gamma'\frac{\partial\psi}{\partial z}\right]\right.$$

$$+ 2y\left[(\alpha + 2x^2\alpha' + 2xy\beta')\frac{\partial\psi}{\partial x} + (2xy\alpha' - \beta - 2x^2\beta')\frac{\partial\psi}{\partial y} + 2x\gamma'\frac{\partial\psi}{\partial z}\right]$$

$$- x\psi\frac{\partial}{\partial y}\left(2\alpha + 2x^2\alpha' + 2xy\beta' + 2y^2\alpha' - 2xy\beta' + \frac{\partial\gamma}{\partial z}\right)$$

$$\left. + y\psi\frac{\partial}{\partial x}\left(2\alpha + 2x^2\alpha' + 2xy\beta' + 2y^2\alpha' - 2xy\beta' + \frac{\partial\gamma}{\partial z}\right)\right\}$$

$$- x\psi(4x^2y\alpha\alpha' + 2y\beta^2 + 4y^3\beta\beta' + 2y\alpha^2 + 4y^3\alpha\alpha' + 4x^2y\beta\beta' + 4y\gamma\gamma')$$

$$+ y\psi(2x\alpha^2 + 4x^3\alpha\alpha' + 4xy^2\beta\beta' + 4xy^2\alpha\alpha' + 2x\beta^2 + 4x^3\beta\beta' + 4x\gamma\gamma').$$

This simplifies to

$$[\hat{H},\hat{L}_z]\psi = ix\psi\frac{\partial}{\partial y}\left(2\alpha + 2x^2\alpha' + 2y^2\alpha' + \frac{\partial\gamma}{\partial z}\right) - iy\psi\frac{\partial}{\partial x}\left(2\alpha + 2x^2\alpha' + 2y^2\alpha' + \frac{\partial\gamma}{\partial z}\right)$$

$$= i\left(4xy\alpha' + 4x^3y\alpha'' + 4xy\alpha' + 4xy^3\alpha'' + 2xy\frac{\partial\gamma'}{\partial z} - 4xy\alpha' - 4xy\alpha' - 4x^3y\alpha'' - 4xy^3\alpha'' - 2xy\frac{\partial\gamma'}{\partial z}\right)$$

$$= 0.$$

Thus, the vector potentials of the form (B27) fulfill the condition $[\hat{H},\hat{L}_z] = 0$ and in these gauges $\hat{L}_z$ is a constant of motion.

3. Gauge transformations between vector potentials for which L_z is a constant of motion

We now consider a gauge transformation between two gauges of the form (B27). A vector potential of this form gives the magnetic field

$$\mathbf{B} = \nabla \times \mathbf{A}$$

$$= \nabla \times [x\alpha + y\beta, y\alpha - x\beta, \gamma] = \left[2y\gamma' - y\frac{\partial\alpha}{\partial z} + x\frac{\partial\beta}{\partial z}, x\frac{\partial\alpha}{\partial z} + y\frac{\partial\beta}{\partial z} - 2x\gamma', 2xy\alpha' - \beta - 2x^2\beta' - 2xy\alpha' - \beta - 2y^2\beta'\right]$$

$$= \left[2y\gamma' - y\frac{\partial\alpha}{\partial z} + x\frac{\partial\beta}{\partial z}, x\frac{\partial\alpha}{\partial z} + y\frac{\partial\beta}{\partial z} - 2x\gamma', -2\beta - (2x^2 + 2y^2)\beta'\right].$$

Since any modification to β would affect the -2β term in the z component of **B** and **B** must be unchanged by gauge transformations, β must be constant in a gauge transformation.

A gauge transformation is given by $\mathbf{A}' = \mathbf{A} + \nabla\chi$ and takes the form

$$\nabla\chi = \mathbf{A}' - \mathbf{A},$$
$$= [x\Delta\alpha + y\Delta\beta, y\Delta\alpha - x\Delta\beta, \Delta\gamma]$$
$$= [x\Delta\alpha, y\Delta\alpha, \Delta\gamma], \qquad (B28)$$

using that $\Delta\beta$ must be zero. We obtain χ by integrating each of the components of the vector (B28):

$$\int x\Delta\alpha \, dx = \frac{\lambda(x^2 + y^2, z)}{2},$$

$$\int y\Delta\alpha \, dy = \frac{\mu(x^2 + y^2, z)}{2},$$

$$\int \Delta\gamma \, dz = \nu(x^2 + y^2, z).$$

Clearly then, the scalar field χ must be a function of the form $\chi(x^2 + y^2, z)$.

Finally, we demonstrate that $[\mathbf{r} \times \mathbf{j}_p]_z$ is unchanged by gauge transformations between gauges of the form (B27). The paramagnetic current density transforms according to $\mathbf{j}'_p = \mathbf{j}_p + \rho\nabla\chi$,

$$[\mathbf{r} \times \mathbf{j}'_p]_z = [\mathbf{r} \times (\mathbf{j}_p + \rho\nabla\chi)]_z$$
$$= [\mathbf{r} \times \mathbf{j}_p]_z + [\mathbf{r} \times \rho\nabla\chi]_z$$
$$= [\mathbf{r} \times \mathbf{j}_p]_z + [\mathbf{r} \times \rho[x\Delta\alpha, y\Delta\alpha, \Delta\gamma]]_z$$
$$= [\mathbf{r} \times \mathbf{j}_p]_z + \rho[xy\Delta\alpha - xy\Delta\alpha]$$
$$= [\mathbf{r} \times \mathbf{j}_p]_z.$$

So, when we are in any gauge of the form of Eq. (B27) and when we transform between any of these gauges, both $\hat{L}_z$ and $[\mathbf{r} \times \mathbf{j}_p]_z$ are unaffected.

[1] A. Thirumalai and J. S. Heyl, Hydrogen and helium atoms in strong magnetic fields, Phys. Rev. A **79**, 012514 (2009).

[2] A. Thirumalai, S. J. Desch, and P. Young, Carbon atom in intense magnetic fields, Phys. Rev. A **90**, 052501 (2014).

[3] M. Mehring, J. Mende, and W. Scherer, Entanglement between an electron and a nuclear spin $\frac{1}{2}$, Phys. Rev. Lett. **90**, 153001 (2003).

[4] S. Takahashi, R. Hanson, J. van Tol, M. Sherwin, and D. Awschalom, Quenching spin decoherence in diamond through spin bath polarization, Phys. Rev. Lett. **101**, 047601 (2008).

[5] I. D'Amico, J. P. Coe, V. V. França, and K. Capelle, Quantum mechanics in metric space: Wave functions and their densities, Phys. Rev. Lett. **106**, 050401 (2011).

[6] E. Artacho, Comment on Quantum mechanics in metric space: Wave functions and their densities, Phys. Rev. Lett. **107**, 188901 (2011).

[7] I. D'Amico, J. P. Coe, V. V. França, and K. Capelle, D'Amico *et al.* Reply, Phys. Rev. Lett. **107**, 188902 (2011).

[8] P. M. Sharp and I. D'Amico, Metric space formulation of quantum mechanical conservation laws, Phys. Rev. B **89**, 115137 (2014).

[9] M. Taut, P. Machon, and H. Eschrig, Violation of noninteracting $\mathcal{V}$-representability of the exact solutions of the Schrödinger equation for a two-electron quantum dot in a homogeneous magnetic field, Phys. Rev. A **80**, 022517 (2009).

[10] E. I. Tellgren, S. Kvaal, E. Sagvolden, U. Ekström, A. M. Teale, and T. Helgaker, Choice of basic variables in current-density-functional theory, Phys. Rev. A **86**, 062506 (2012).

[11] E. H. Lieb and R. Schrader, Current densities in density-functional theory, Phys. Rev. A **88**, 032516 (2013).

[12] E. I. Tellgren, S. Kvaal, and T. Helgaker, Fermion n-representability for prescribed density and paramagnetic current density, Phys. Rev. A **89**, 012515 (2014).

[13] A. Laestadius and M. Benedicks, Nonexistence of a Hohenberg-Kohn variational principle in total current-density-functional theory, Phys. Rev. A **91**, 032508 (2015).

[14] I. Nagy and I. Aldazabal, Metric measures of interparticle interaction in an exactly solvable two-electron model atom, Phys. Rev. A **84**, 032516 (2011).

[15] W. A. Sutherland, *Introduction to Metric & Topological Spaces* (Oxford University Press, Oxford, 2009).

[16] R. E. Megginson, *An Introduction to Banach Space Theory* (Springer, Berlin, 1998).

[17] G. Vignale and Mark Rasolt, Density-functional theory in strong magnetic fields, Phys. Rev. Lett. **59**, 2360 (1987).

[18] C. Cohen-Tannoudji, B. Diu, and F. Laloë, *Quantum Mechanics* (Wiley, New York, 1977).

[19] M. Taut, Two electrons in a homogeneous magnetic field: Particular analytical solutions, J. Phys. A **27**, 1045 (1994).

[20] L. Quiroga, D. R. Ardila, and N. F. Johnson, Spatial correlation of quantum dot electrons in a magnetic field, Solid State Commun. **86**, 775 (1993).

[21] J. P. Coe, A. Sudbery, and I. D'Amico, Entanglement and density-functional theory: Testing approximations on Hooke's atom, Phys. Rev. B **77**, 205122 (2008).

[22] K. Capelle, A bird's-eye view of density-functional theory, Braz. J. Phys. **36**, 1318 12 (2006).

[23] C. A. Ullrich and Z. Yang, A brief compendium of time-dependent density functional theory, Braz. J Phys. **44**, 154 (2013).

[24] P. Hohenberg and W. Kohn, Inhomogeneous electron gas, Phys. Rev. **136**, B864 (1964).

[25] C. S. Kubrusly, *The Elements of Operator Theory* (Springer, Berlin, 2009).

[26] D. Burago, Y. Burago, and S. Ivanov, *A Course in Metric Geometry* (American Mathematical Society, Providence, 2001).

[27] L. Longpré and V. Kreinovich, When are two wave functions distinguishable: A new answer to Pauli's question, with potential application to quantum cosmology, Int. J. Theor. Phys. **47**, 814 (2008).

[28] H.-K. Rhee, R. Aris, and N. R. Amundson, *First Order Partial Differential Equations* (David & Charles, Newton Abbot, 2001).

[29] E. Kreyzig, *Advanced Engineering Mathematics* (Wiley, New York, 2006).

[30] I. S. Gradshteyn and I. M. Ryzhik, *Table of Integrals, Series and Products* (Academic Press, New York, 2000).